中国光学（中英文）
Chinese Optics
核心期刊

**奇偶探测超分辨率折射率测量的理论研究**

王强 王倩倩 王振 郝利丽

**Theoretical investigation on super-resolution refractive index measurement with parity detection**

WANG Qiang, WANG Qian-qian, WANG Zhen, HAO Li-li

引用本文:
王强, 王倩倩, 王振, 郝利丽. 奇偶探测超分辨率折射率测量的理论研究[J]. 中国光学, 2023, 16(2): 434-446. doi: 10.37188/CO.2022-0119
WANG Qiang, WANG Qian-qian, WANG Zhen, HAO Li-li. Theoretical investigation on super-resolution refractive index measurement with parity detection[J]. *Chinese Optics*, 2023, 16(2): 434-446. doi: 10.37188/CO.2022-0119

在线阅读 View online: https://doi.org/10.37188/CO.2022-0119

文章编号　2097-1842(2023)02-0434-13

# Theoretical investigation on super-resolution refractive index measurement with parity detection

WANG Qiang, WANG Qian-qian, WANG Zhen, HAO Li-li*
(*School of Physics and Electronic Engineering*, *Northeast Petroleum University*, *Daqing* 163318, *China*)
* *Corresponding author*, *E-mail*: *haolili*0820@126.*com*

**Abstract**: The refractive index measurements based on traditional wave optical methods are mainly depended on intensity and wavelength detection strategies. Interference spectrometers are widely used as the most ideal wavelength detecting devices. Interference spectrometers measure the signal intensity, analyze the change of fringe numbers and the corresponding optical path difference by means of optical power meter, and then calculate the wavelength of signal light. Therefore, its essence is still based on intensity detection. However, the resolution of interference signal in intensity detection is restricted by classical diffraction limit, thus its resolution is difficult to further improve. In order to solve this bottleneck, parity detection which could break through the classical resolution limit and realize super-resolution refractive index measurement is proposed in this paper. According to the quantum detection and estimation theory, the expressions for signals and their corresponding sensitivities of refractive index measurement with parity and intensity detections were derived respectively and their numerical comparison analysis was carried out. In addition, the effects of loss on resolution and sensitivity of the output signal were investigated. Numerical results show that the resolution of parity detection is $2\pi\sqrt{N}$ times that of intensity detection, achieving super-resolution refractive index measurement. Moreover, the optimal sensitivity reaches the refractive index measurement shot noise limit $\lambda\Big/\left(2\pi l\sqrt{N}\right)$. The loss reduces the sensitivity and resolution of the signal. The resolution of the parity detection signal is consistently better than that of intensity detection except for the very large loss and very low photon number. Finally, the physical essence of the super-resolution refractive index measurement is analyzed from the detection means itself.

**Key words**: refractive index measurement; parity detection; diffractive limit; super-resolution

收稿日期:2022-06-10; 修订日期:2022-07-13

基金项目:东北石油大学引导性创新基金(No. 2021YDL-16);黑龙江省教育规划重点课题(No. GJB1320038, No. GJB1422173);东北石油大学教育教学改革项目(No. JGXM_NEPU_202114)

Supported by Guiding Innovation Fund of Northeast Petroleum University (No. 2021YDL-16); Heilongjiang Province Education Planning Key Project (No. GJB1320038 , No. GJB1422173); The Education Teaching Reform Project of Northeast Petroleum University (No. JGXM_NEPU_202114)

# 奇偶探测超分辨率折射率测量的理论研究

王　强, 王倩倩, 王　振, 郝利丽*

（东北石油大学 物理与电子工程学院，黑龙江 大庆 163318）

**摘要:** 传统波动光学法测量样品折射率所采用的探测方法主要是强度探测和波长探测。波长的最佳检测器件为干涉型光谱仪，干涉型光谱仪是通过光功率计测量信号强度、分析条纹数目变化及所对应的光程差，进而计算出信号光波长，因此，其本质仍是以强度探测为基础的。然而，利用强度探测干涉信号，分辨率受经典衍射极限限制，很难得到进一步提升。为了解决这一瓶颈问题，本文提出利用奇偶探测突破经典分辨率的极限限制，实现超分辨率折射率测量。根据量子探测与估计理论，推导了奇偶探测和强度探测折射率测量信号及其灵敏度表达式，并进行了数值对比分析。同时，研究了损耗对系统输出信号分辨率和灵敏度的影响。数值结果表明: 奇偶探测分辨率是强度探测的$2\pi\sqrt{N}$倍，实现了超分辨率折射率测量，最佳灵敏度达到了折射率测量散弹噪声极限$\lambda/(2\pi l\sqrt{N})$，损耗降低了信号的分辨率和灵敏度，除极大损耗和极低光子数外，奇偶探测信号分辨率始终优于强度探测。最后，从探测手段本身出发分析了奇偶探测超分辨率折射射率测量的物理本质。

**关　键　词:** 折射率测量; 奇偶探测; 衍射极限; 超分辨率

**中图分类号:** O436.1;TN249　　**文献标志码:** A　　**doi:** 10.37188/CO.2022-0119

## 1　Introduction

Refractive index is an important optical parameter of transparent and translucent materials, which reflects the inherent properties of the substance and is mainly used in biomedicine, environmental monitoring, petrochemicals, and food processing, etc.[1]. The measurement of refractive index allows the detection of relevant indicators of a sample: for example, obtaining the salinity of seawater [2], analyzing the contamination of seawater [3], and determining the quality of food [4]. The traditional refractive index measurement methods are divided into geometric optical method and wave optics method. The geometric optical method has low measurement accuracy [5-7], poor stability [8], difficult mechanical processing, expensive cost [9], and requires high processing accuracy [10]. Therefore, the geometric optical method is commonly used in the field of refractive index measurement, which does not require high accuracy.

Wave optics methods include wedge interferometry [11], Michelson interferometry [12], Fabry-Perot interferometry [13-14], Newton's Rings interferometry [15], photonic crystal fiber method based on surface plasmon resonance [16] and optical frequency comb [17]. The wave optics method is widely used in refractive index measurements because of its advantages such as anti-electromagnetic interference, compact size, low cost and low loss [18]. The wave optics method uses two main detection methods, namely intensity detection and wavelength detection. The wavelength detection takes the Optical Spectrum Analyzer (OSA) as the main detection device, and the OSA with better performance generally adopts the interferometric method to measure the number of interference fringes and the corresponding optical path difference to obtain the incident light wavelength, and its essence is to detect the intensity change of interference fringes, count the number of fringes, and finally calculate the corresponding wavelength by the optical power meter. In this sense, OSA is also a wavelength detection device based on intensity detection. However, the signal resolution and sensitivity of the conventional intensity detection are limited by the Rayleigh diffraction limit and the shot noise limit, and it is difficult to further improve the detection performance. Since the work of Boto et al. [19] was reported, the use of quantum phenomena and detection methods[20] to break the limit of Rayleigh diffraction and thus improve the performance of interferometric sensing systems has become a paradigm in the field of interferometric sensing and remote sensing. Therefore, the use of quantum phenomena, quantum detection methods and data post-processing means are expected to break through the limit of refractive index measurements and achieve super-resolution refractive index measurements.

A scheme for super-resolution refractive index measurement using parity detection is proposed in the paper. The refractive index measurement resolution of this detection scheme break through the Rayleigh diffraction limit, thus achieving super-resolution refractive index measurement. The intensity-detection-based refractive index measurement is also investigated in the paper. Theoretical derivation and numerical analysis show that: the intensity detection resolution is the Refractive Index Measurement-Rayleigh Diffraction Limit (RIM-RDL), and the sensitivity reaches the Refractive Index Measurement-Shot Noise Limit (RIM-SNL); the parity detection signal resolution is $2\pi\sqrt{N}$ times of RIM-RDL, and the sensitivity reaches RIM-SNL, except for the very large loss and very low photon number, the parity detection resolution has broken through the RIM-RDL limit. More importantly, the physical nature of the super-resolution of parity detection is discussed in detail.

## 2 Measurement principle

The measurement principle of super-resolution refractive index using parity detection is similar to the classical Mach-Zehnder Interferometer (MZI), as shown in Fig. 1. In Fig.1, BS stands for Beam Splitter, M stands for plane mirror, B($T$) stands for virtual beam splitter, which is used to simulate photon number loss, and RIS($n$) stands for Refractive Index Shift (RIS), which is used to continuously change the refractive index of the measured sample (the refractive index of the sample can be changed by heating, illumination or electric action), where $n$ is the refractive index of the sample.

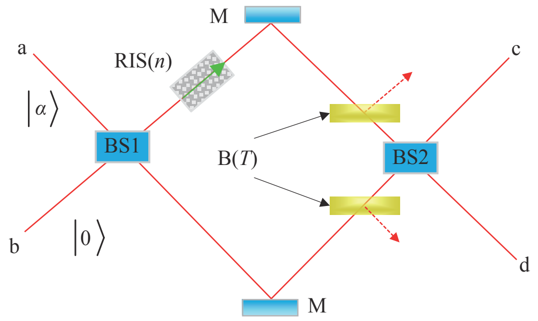


Fig. 1 Schematic diagram of super-resolution refractive index measurement principle using parity detection

图 1 奇偶探测超分辨率折射率测量原理示意图

The coherent state $|\alpha\rangle$ is injected into the interferometer from incident port a of the MZI, while the vacuum state $|0\rangle$ is incident from port b. The two quantum state beams are acted upon by BS1, and the beam propagating along the clockwise direction produces a phase shift $\varphi(n)=k(n-1)l$ via RIS($n$), where $l$ is the length of the measured sample along the beam propagation direction and $k$ is the incident light wave number. The beam, after the loss and the reflection by the plane mirror M, meets and interferes with the loss-propagated beam propagating in the counter clockwise direction at BS2. The interference signals are received, detected and post-processed at the exit ports c and d. The refractive index of the sample is estimated according to the quantum detection and estimation theory, and the detection performance of the system is evaluated.

## 3 Intensity-detection-based refractive index measurement

According to the theory of quantum optics, the direct product state $\psi_{\rm in}=|\alpha\rangle\otimes|0\rangle$ of coherent state and vacuum state is used as the input state of MZI, and the output state after passing beam splitter BS1 is

$$\psi_{\rm I}=\left|\alpha/\sqrt{2}\right\rangle\left|\alpha/\sqrt{2}\right\rangle \quad . \tag{1}$$

This state has a phase shift $\varphi(n)$ due to the change in refractive index of the sample in one of its paths, and both paths experience photon loss. The state after loss and phase shift is

$$\psi_{\mathrm{II}} = \left|\sqrt{T}\alpha/\sqrt{2}\right\rangle \left|\sqrt{T}\alpha e^{-ik(n-1)l}/\sqrt{2}\right\rangle \quad . \tag{2}$$

Two beams meet and interfere at BS2, and the output bimodal quantum state after the interference can be expressed as

$$\psi_{\mathrm{out}} = \left|\alpha\sqrt{T}\left(e^{-ik(n-1)l}-1\right)/2\right\rangle \left|\alpha\sqrt{T}\left(e^{ik(n-1)l}+1\right)/2\right\rangle \quad . \tag{3}$$

The intensity detection is implemented at one output of the MZI, i.e., the intensity signal at this output is $I = \langle \hat{I} \rangle = {}_{\mathrm{out}}\langle\psi|\hat{a}^{+}\hat{a}|\psi\rangle_{\mathrm{out}}$, where $\hat{a}^{\dagger}$ and $\hat{a}$ are the creation-annihilation operators at the output, respectively. After calculation, we obtain

$$I = TN\cos^2[l\pi(n-1)/\lambda] \quad , \tag{4}$$

where $N = |\alpha|^2$ is the average photon number of the incident coherent state beam, $T$ is the photon number transmission rate, and $\lambda$ is the incident light wavelength.

According to the expression of Eq. (4), it can be analyzed that the intensity-detection-based interferometric signal resolution can be approximated by the period $\Delta n_{\mathrm{I}} = \lambda/l$ of the signal, similar to the classical Rayleigh diffraction limit $\lambda/2$, which is defined here as the RIM-RDL. Therefore, the resolution limits of conventional intensity- and wavelength-based detection refractive index measurements are both $\lambda/l$. In addition, Eq. (4) also shows that the intensity-detection-based signal resolution is not affected by photon number and loss, which only affect the signal amplitude.

The sensitivity of the intensity-detection-based refractive index measurement signal can be calculated from Eq. (4) and the intensity-detection-based Gaussian error propagation formula $\delta n_{\mathrm{I}} = \sqrt{\langle \hat{I}^2 \rangle - \langle \hat{I} \rangle^2} / \left|\partial\langle \hat{I} \rangle/\partial n\right|$. Firstly, the average value of the intensity operator squared is calculated as

$$\begin{aligned}\langle \hat{I}^2 \rangle &= {}_{\mathrm{out}}\langle\psi|\hat{a}^{+}\hat{a}\hat{a}^{+}\hat{a}|\psi\rangle_{\mathrm{out}} \\ &= N^2T^2\cos^4\left[l\pi(n-1)/\lambda\right] + NT\cos^2[l\pi(n-1)/\lambda] \quad .\end{aligned} \tag{5}$$

Secondly, calculate the partial derivative of the intensity detection signal to the refractive index as

$$\left|\partial\langle \hat{I} \rangle/\partial n\right| = |TN\pi l\sin[2l\pi(n-1)/\lambda]/\lambda| \quad . \tag{6}$$

Finally, substituting Eq. (5) and Eq. (6) into the intensity-detection-based Gaussian error propagation formula, the sensitivity of the signal can be obtained as

$$\delta n_{\mathrm{I}} = \frac{\lambda}{2\sqrt{TN}\pi l|\sin[l\pi(n-1)/\lambda]|} \quad . \tag{7}$$

From Eq. (7), we get $\delta n_{\mathrm{I}} \geqslant \lambda/\left(2\pi l\sqrt{TN}\right)$. This result indicates that the minimum value of the sensitivity of the refractive index measurement based on intensity detection is $\lambda/\left(2\pi l\sqrt{N}\right)$. This phenomenon is similar to the shot noise limit $1/\sqrt{N}$. Similarly, this sensitivity is defined as Refractive Index Measurement Shot Noise Limit (RIM-SNL). In principle, the sensitivity of the refractive index measurement signal is limited by this limit for both direct and indirect applications of intensity detection.

Fig. 2 (color online) illustrates the sensitivity curve of the signal for intensity detection refractive index measurement and the effect of photon number and transmittance on the optimal sensitivity (minimum value of sensitivity), where $\lambda$=532 nm and $l$=5.3 mm. Fig. 2(a) represents the curve of signal sensitivity with medium refractive index, where the average photon number $N$=10 and transmittance $T$=1. Fig. 2(b) characterizes output signal optimal sensitivity as a function of photon number and transmittance. From Fig. 2 (b), it can be seen that the optimal sensitivity of the signal increases with the increase of photon number, and the loss of photon number decreases the optimal sensitivity of the signal.

The above analysis shows that the sensitivity of the signal can be improved by appropriately increasing the number of incident light photons (power), but the resolution of the signal is independent of the number of photons. Increasing the signal transmittance (reducing the loss) can improve the signal sensitivity, but also has no effect on the signal resolution. However, the improvement of system performance by increasing photon number and transmittance is still limited to the classical intensity detection framework, and the resolution and sensitivity of refractive index measurement are still limited by RIM-RDL and RIM-SNL, and it is difficult to further improve the resolution and sensitivity. Therefore, it is necessary to innovate the detection system to break through the RIM-RDL and RIM-SNL limitations and thus improve the system detection performance.

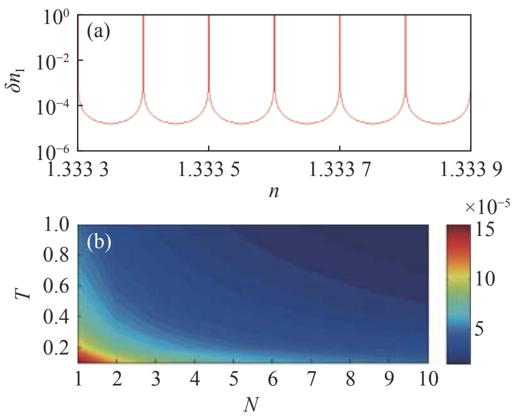


Fig. 2 (a) Sensitivity curve of intensity-detection-based refractive index measurement and (b) signal optimal sensitivity as a function of photon number and transmittance

图 2 (a) 强度探测折射率测量灵敏度曲线及 (b) 信号最佳灵敏度随光子数和透过率的变化关系

## 4 Refractive index measurement using parity detection

Parity detection was first proposed by Bollinger[21] when studying trapped ions, and then, Gerry *et al.*[22] implemented phase measurements based on the concept of parity detection, and the results of the study broke through the classical resolution and sensitivity limits to achieve super-resolution and super-sensitivity phase measurements. For most of the quantum states, parity detection is the best detection scheme for parameter estimation. The parity detection operator $\hat{\Pi} = \mathrm{e}^{\mathrm{i}\hat{N}\pi}$ ($\hat{N} = \hat{a}^{\dagger}\hat{a}$ is the particle number operator) is closely related to the Wigner Function, which is exactly the average value of the displacement parity operator, and the average value of the parity detection signal can be calculated by the relationship between the Wigner Function of the MZI input and output states. For input state $|\alpha\rangle\langle\alpha|\otimes|0\rangle\langle 0|$, its Wigner function can be expressed as

$$W_{\mathrm{in}}(\gamma,\beta) = W_{|\alpha\rangle}(\gamma)\,W_{|0\rangle}(\beta) \quad , \tag{8}$$

where $W_{|\alpha\rangle}(\gamma)$ and $W_{|0\rangle}(\beta)$ are the Wigner functions for the coherent and vacuum states, respectively, and their expressions are

$$W_{|\alpha\rangle}(\gamma) = \frac{2}{\pi}\mathrm{e}^{-2|\gamma-\alpha|^2} \quad , \tag{9}$$

$$W_{|0\rangle}(\beta) = \frac{2}{\pi}\mathrm{e}^{-2|\beta|^2} \quad . \tag{10}$$

The transformation relation between the input and output Wegener functions can be realized by the following transformation:

$$W_{\mathrm{out}}(\gamma,\beta) = W_{\mathrm{in}}\left(\tilde{\gamma},\tilde{\beta}\right) \quad , \tag{11}$$

where $\tilde{\gamma} = \gamma\cos[\pi l(n-1)/\lambda] + \beta\sin[\pi l(n-1)/\lambda]$ and $\tilde{\beta} = -\gamma\sin[\pi l(n-1)/\lambda] + \beta\cos[\pi l(n-1)/\lambda]$.

Thus, the average value of the parity detection operator can be expressed as

$$\left\langle\hat{\Pi}\right\rangle = \frac{\pi}{2}\int_{-\infty}^{\infty} W_{\mathrm{out}}(0,\beta)\,\mathrm{d}^2\beta \quad . \tag{12}$$

After considering the photon number loss, the specific expression for the average value of the parity detection signal can be deduced from the above analysis as

$$\left\langle\hat{\Pi}\right\rangle = \mathrm{e}^{-2TN\sin^2[\pi l(n-1)/\lambda]} \quad . \tag{13}$$

According to Eq. (13), the parity detection signal curve is plotted in Fig. 3 (color online) as shown by the red dotted line, and the intensity detection signal curve is also plotted in Fig. 3 as shown by the black solid line using Eq. (4). It can be seen from Fig. 3 that the Full Width of Half Maximum (FWHM) of the parity detection signal is significantly smaller than the FWHM of the intensity detection, which indicates that the resolution of the parity detection signal is better than that of the intensity detection. In order to further give a quantitative relationship between the intensity detection and parity detection signal resolution, we use a similar small-angle approximation method to make an approximation to Eq. (13), i.e., when $\pi l(n-1)/\lambda \ll 1$, Eq. (13) can be approximated as

$$\langle\hat{\Pi}\rangle = \mathrm{e}^{-2TN(\pi l/\lambda)^2(n-1)^2} \quad . \tag{14}$$

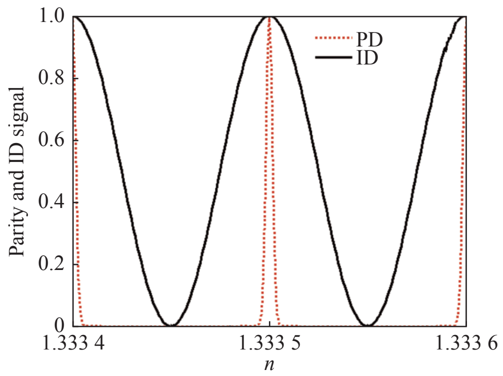


Fig. 3　Signals of parity detection and normalized intensity detection are plotted as a function of refractive index $n$ for the average photon number of $N = 100$. The red dotted line and black solid line represent parity detection (PD) and normalized intensity detection (ID) respectively

图 3　奇偶探测信号和归一化强度探测信号随折射率 $n$ 的变化，输入信号的平均光子数$N = 100$，红色点线和黑色实线分别代表奇偶探测信号和归一化强度探测信号

The above approximation shows that this signal has Gaussian distribution characteristics, then the width of this signal is $\Delta n_{\mathrm{P}} = \lambda/\left(2\pi l\sqrt{TN}\right)$. According to the previous discussion, the resolution of the intensity detection signal is approximated as $\Delta n_{\mathrm{I}} = \lambda/l$, when $T = 1$, the intensity detection signal peak is $2\pi\sqrt{N}$ times wider than the parity detection signal peak, which means that the resolution of the parity detection signal is $2\pi\sqrt{N}$ times higher than the intensity detection. Therefore, super-resolution refractive index measurements beyond the RIM-RDL limits can be realized theoretically by parity detection.

In practical applications, losses are unavoidable. Fig. 4 (color online) plots the FWHM of the parity detection signal varies with transmittance and photon number, as shown by the red dotted line, where $\lambda$ = 532 nm and $l$ = 1 064 nm. For comparison, the FWHM of the intensity detection signal varying with transmittance and photon number under the same conditions is also given in the figure, as shown by the blue solid line. It is obvious from the figure that the resolution of the intensity detection signal is independent of the transmittance and photon number, which is consistent with the previous analysis. It can also be seen that the resolution of the parity detection signal decreases with the increase of the loss (decreasing transmittance) and the decrease of the photon number. Only when the average photon number $N$ < 1.1 and transmittance $T$ < 0.011, the resolution of the parity detection signal is lower than that of the intensity detection, and the resolution of the parity detection signal is much higher than that of the intensity detection in all other cases. Therefore, except for the case of very low photon number and very high loss, the resolution of the parity detection signal is higher than that of the intensity detection.

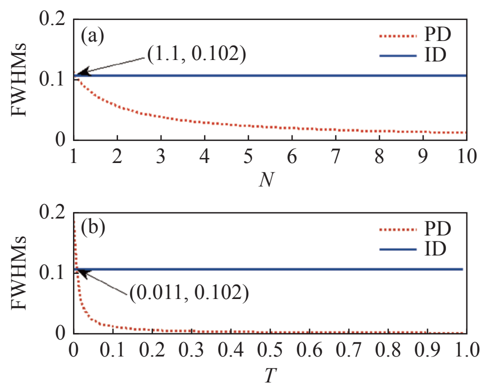


Fig. 4　FWHMs of parity and intensity detections varying with the average photon number (a) and transmittance (b)

图 4　奇偶探测和强度探测的 FWHMs 随着平均光子数 (a) 和透过率 (b) 的变化规律

The sensitivity of the parity detection signal can be deduced from the Gaussian error transfer equation $\delta n_{\mathrm{P}} = \sqrt{\langle\hat{\Pi}^2\rangle - \langle\hat{\Pi}\rangle^2}\Big/\left|\partial\langle\hat{\Pi}\rangle/\partial n\right|$ for the parity detection signal. First, according to Eq. (13) and $\langle\hat{\Pi}^2\rangle = 1$, the expression of the uncertainty of the parity detection signal $\Delta\Pi = \sqrt{1-\langle\hat{\Pi}\rangle^2} =$

$\sqrt{1-e^{-4TN\sin^2[\pi l(n-1)/\lambda]}}$ can be obtained, and then the partial derivative of the parity detection signal with respect to the refractive index $\left|\partial\langle\hat{\Pi}\rangle/\partial n\right| = \frac{2TN\pi l}{\lambda}\left|\sin\left[\frac{2l\pi(n-1)}{\lambda}\right]\right| e^{\left\{-2TN\sin^2\left[\frac{l\pi(n-1)}{\lambda}\right]\right\}}$ is calculated, and finally, the expression of the sensitivity of the parity detection signal can be derived from the Gaussian error transfer formula of the parity detection

$$\delta n_{\mathrm{P}} = \frac{\lambda}{2TN\pi l}\frac{\sqrt{e^{4TN\sin^2[l\pi(n-1)/\lambda]}-1}}{|\sin[2l\pi(n-1)/\lambda]|} . \tag{15}$$

According to Eq. (15), the parity detection signal sensitivity curve is obtained numerically as shown in Fig. 5 (color online), where $\lambda = 532$ nm, $l =$ 5.3 mm, $N = 100$. The red dotted line in the figure shows the parity detection signal sensitivity curve. Also, for comparative analysis, the sensitivity curves of the intensity detection signal are given in the figure, as shown by the blue solid line in the figure. The black straight dashed line in the figure is the tangent line of the two curves. The tangent line of the two sensitivity curves is a straight line, indicating that the best sensitivity of the signal is the same for both detection methods. This common tangent line is also the RIM-SNL under the above conditions, i.e., the parity detection refractive index measurement is a super-resolution detection scheme based on RIM-SNL.

Next, the effects of photon number and transmittance on the optimal sensitivity of the signal are considered. Fig. 6(a) and Fig. 6(b) (color online) show the effect of transmittance and photon number on the optimal sensitivity of the signal for parity detection and intensity detection, respectively, where $\lambda$ =532 nm, $l$ =5.3mm . The optimal sensitivity of the signal increases with the increase of photon number and transmittance for both detection methods, and more importantly, the two curves always coincide in both cases, which indicates that the optimal sensitivity is the same for both detections. In other words, compared to intensity detection, parity detection cannot further improve the sensitivity of refractive index measurement.

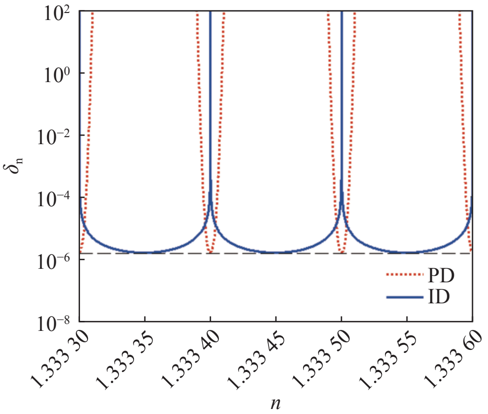


Fig. 5 Sensitivity curves of parity detection (red dotted line) and intensity detection (blue solid line), and the black dashed line represents their common tangents

图 5 奇偶探测(红色点线)和强度探测(蓝色实线)信号灵敏度曲线,黑色虚线为两条曲线的公切线

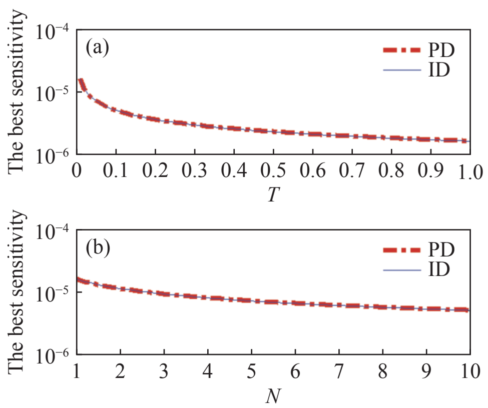


Fig. 6 Optimal sensitivity of parity detection and intensity detection signals varying with transmittance (a) and photon number (b). The red dot dashed line indicates parity detection and the blue solid line represents intensity detection

图 6 奇偶探测和强度探测信号最佳灵敏度随着透过率 (a) 和光子数 (b) 的变化曲线,红色点虚线表示奇偶探测,蓝色实线代表强度探测

It is known from the previous discussion that the parity detection signal can break RIM-RDL, and the sensitivity can reach RIM-SNL. However, the physical nature of the super-resolution of parity detection refractive index measurement is still unclear, so further analysis of the nature of the parity detection refractive index measurement is necessary and essential.

The interference principles followed in the paper based on intensity detection and parity detection refractive index measurements are based on Mach-Zehnder interferometer, and the input light is a coherent state beam, so the resolution improvement is not related to the interferometer and the input state beam. Then, the resolution improvement can only be related to the detection method and post-processing method at the output of the system. Intensity detection is a traditional detection method for direct detection of the intensity of the optical signal at the output of the system, and its resolution depends on the classical Rayleigh diffraction limit, and the resolution cannot be further improved. However, parity detection is a further post-processing of the optical signal at the output, that is, the number of photons in the output optical field is classified, and the probabilities of even and odd number of photons in the output are counted separately, and then the statistical distribution of this parity is given, and the average value of the parity detection operator is derived to obtain the parity detection signal. This measurement scheme is equivalent to projecting the measured output state onto an even photon number state or an odd photon number state, i.e., to obtain an infinitely compressed quantum state[23-24] which is capable of improving the signal measurement resolution. In summary, the nature of the parity detection signal resolution enhancement becomes quite clear. This interpretation is similar to the super-resolution parameter estimation performed directly using the compressed state, with the difference that the data post-processing is utilized instead of the compressed state, avoiding the tedious preparation of the compressed state.

## 5 Conclusion

In this paper, a super-resolution refractive index measurement scheme using parity detection is proposed to address the bottleneck problem of the resolution of conventional refractive index measurement. The intensity detection, parity detection refractive measurement signal models and their sensitivity models based on quantum theory are derived. In addition, from the intensity detection model itself, this paper analyzes the intensity detection model on its signal period, and thus defines the intensity detection signal resolution limit and sensitivity limit. The intensity-detection and parity detection refractive index measurement signal are compared and analyzed by a combination of model analysis and numerical methods. The results show that the sensitivity of both detection schemes can reach RIM-SNL; the resolution of the parity detection signal is much higher than RDL, which is $2\pi\sqrt{N}$ times higher than the resolution of the intensity detection signal. At the same time, the resolution of parity detection exceeds that of intensity detection in almost the entire loss region. Finally, parity detection is equivalent to projecting the output state into an infinitely compressed state with an even or odd number of photons, and the infinite compression will inevitably increase the resolution of the measured signal. This scheme opens a way to break through the limit of classical resolution detection and provides a new method for super-resolution refractive index measurement.

——中文对照版——

## 1 引　言

折射率是透明材料和半透明材料的一个重要光学参数，反映了物质的固有属性，在生物医药、环境监测、石油化工、食品加工等领域均有重要应用[1]。通过测量折射率可以检测样品的相关指标：如获得海水盐度[2]、分析海水污染情况[3]，判断食品品质[4]等。传统的折射率测量方法分为几何光学法和波动光学法。几何光学法测量精度较低[5-7]、稳定性差[8]、机械加工困难、成本昂贵[9]，同时对加工精度要求较高[10]。因此，几何光学法普遍应用于对精度要求不高的折射率测量领域。

波动光学法包括劈尖干涉法[11]、迈克尔逊干涉法[12]、法布里-珀罗干涉法[13-14]、牛顿环干涉法[15]、

表面等离子体共振光子晶体光纤法[16] 及光学频率梳[17] 等。波动光学法因具有抗电磁干扰、尺寸小、成本低及损耗低等优势，被广泛地应用于折射率测量领域[18]。波动光学法所采用的测量方式主要是强度探测和波长探测。波长探测以光谱仪（Optical Spectrum Analyzer, OSA) 为主要检测器件，性能较好的 OSA 普遍采用干涉法测量干涉条纹数目和对应的光程差来获取入射光波长，其本质还是通过光功率计探测干涉条纹强度变化、统计条纹数目，最终计算出相应的波长。从这个意义上说，OSA 也是以强度探测为基础的波长检测器件。然而，传统的强度探测信号分辨率和灵敏度受限于瑞利衍射极限和散弹噪声极限，其探测性能很难进一步提升。自从 Boto 等人[19] 的工作被报道以来，利用量子现象及探测方法[20] 突破瑞利衍射极限限制，进而提高干涉传感系统性能，已成为干涉传感及遥感领域的范式。因此，利用量子现象、量子探测方法及数据后处理手段有望突破折射率测量的极限限制，实现超分辨率折射率测量。

文中提出利用奇偶探测实现超分辨率折射率测量方案。该探测方案的折射率测量分辨率突破了瑞利衍射极限，实现了超分辨率折射率测量。同时，文中也对强度探测折射率测量进行了研究。通过理论推导和数值分析可知：强度探测分辨率达到折射率测量瑞利衍射极限 (Refractive Index Measurement Rayleigh Diffraction Limit, RIM-RDL)，灵敏度达到折射率测量散弹噪声极限 (Refractive Index Measurement Shot Noise Limit, RIM-SNL)；奇偶探测信号分辨率是 RIM-RDL 的$2\pi\sqrt{N}$倍，灵敏度达到了 RIM-SNL，除极大损耗和极低光子数外，奇偶探测分辨率均突破了 RIM-RDL 限制。更重要的是奇偶探测超分辨率的物理本质得到了详细讨论。

## 2 测量原理

奇偶探测超分辨率折射率测量原理和经典的马赫-曾德尔干涉仪 (Mach-Zehnder Interferometer, MZI) 相似，如图 1 所示。图中 BS 代表光束分束器 (Beam Splitter, BS)，M 为平面反射镜 (Mirror)，B($T$) 是虚拟分束器，用来模拟光子数损耗，RIS($n$) 表示折射率移动器 (Refractive Index Shift, RIS)，用以连续改变被测样品折射率（可以通过对样品加热，光照或电作用等方式实现样品折射率改变)，其中的 $n$ 为样品的折射率。

相干态$|\alpha\rangle$光束从 MZI 的入射端口 a 射入干涉仪，同时真空态$|0\rangle$从端口 b 入射。两种量子态光束经 BS1 作用后，沿着顺时针方向传播的光束经 RIS($n$) 产生相位移动$\varphi(n)=k(n-1)l$，其中 $l$ 为被测样品沿光束传播方向的长度，$k$ 为入射光波数。该光束经损耗过程和平面镜 M 反射后，与沿逆时针方向传播的经过损耗后的光束在 BS2 处相遇并发生干涉。在出射端口 c 和 d 处对干涉信号进行接收、探测和后处理运算，根据量子探测与估计理论估算样品折射率，评价系统探测性能。

## 3 强度探测折射率测量

根据量子光学理论，将相干态与真空态的直积态$\psi_{\rm in}=|\alpha\rangle\otimes|0\rangle$作为 MZI 的输入态，经过光束分束器 BS1 后的输出态为：

$$\psi_{\rm I}=\left|\alpha/\sqrt{2}\right\rangle\left|\alpha/\sqrt{2}\right\rangle \quad . \tag{1}$$

此状态因其一条路径中样品折射率发生变化而产生相位移动$\varphi(n)$，同时两条路径都经历了光子损耗，则损耗和相移后的状态为：

$$\psi_{\rm II}=\left|\sqrt{T}\alpha/\sqrt{2}\right\rangle\left|\sqrt{T}\alpha{\rm e}^{-{\rm i}k(n-1)l}/\sqrt{2}\right\rangle \quad . \tag{2}$$

两路光束在 BS2 处相遇并干涉，干涉后输出的双模量子态可表示为：

$$\psi_{\rm out}=\left|\alpha\sqrt{T}\left({\rm e}^{-{\rm i}k(n-1)l}-1\right)/2\right\rangle\left|\alpha\sqrt{T}\left({\rm e}^{{\rm i}k(n-1)l}+1\right)/2\right\rangle \quad . \tag{3}$$

在 MZI 的一个输出端实施强度探测，即该输出端的强度信号为$I=\langle\hat{I}\rangle={}_{\rm out}\langle\psi|\hat{a}^{+}\hat{a}|\psi\rangle_{\rm out}$，其中$\hat{a}^{\dagger}$和$\hat{a}$分别为输出端的产生和湮灭算符。经过计算可得：

$$I=TN\cos^{2}[l\pi(n-1)/\lambda] \quad , \tag{4}$$

其中$N=|\alpha|^{2}$为入射相干态光束的平均光子数，$T$为光子数透过率，$\lambda$为入射光波长。

根据公式 (4) 可以分析出强度探测干涉信号分辨率可以用信号的周期$\Delta n_{\rm I}=\lambda/l$近似表征，类似于经典的瑞利衍射极限$\lambda/2$。这里将此分辨率定义为折射率测量的瑞利衍射极限 RIM-RDL。因此，传统的基于强度和波长探测折射率测量的

分辨率极限均为$\lambda/l$。同时,通过公式 (4) 还可以看出强度探测信号分辨率不受光子数和损耗的影响,光子数和损耗只影响信号的幅值。

根据公式 (4) 和强度探测高斯误差传递公式$\delta n_{\mathrm{I}} = \sqrt{\langle \hat{I}^2\rangle - \langle \hat{I}\rangle^2} / \left|\partial\langle \hat{I}\rangle / \partial n\right|$可以计算出强度探测折射率测量信号的灵敏度。首先计算强度算符平方的平均值为:

$$\begin{aligned}\langle \hat{I}^2\rangle &= {}_{\mathrm{out}}\langle\psi|\hat{a}^{+}\hat{a}\hat{a}^{+}\hat{a}|\psi\rangle_{\mathrm{out}} \\ &= N^2T^2\cos^4[l\pi(n-1)/\lambda] + NT\cos^2[l\pi(n-1)/\lambda]\end{aligned} \quad . \tag{5}$$

其次,计算强度探测信号对折射率的偏导数为:

$$\left|\partial\langle \hat{I}\rangle / \partial n\right| = |TN\pi l \sin[2l\pi(n-1)/\lambda]/\lambda| \quad . \tag{6}$$

最后,将公式 (5) 和公式 (6) 代入强度探测信号高斯误差传递公式,可得信号的灵敏度表达式为:

$$\delta n_{\mathrm{I}} = \frac{\lambda}{2\sqrt{TN}\pi l|\sin[l\pi(n-1)/\lambda]|} \quad . \tag{7}$$

由公式 (7) 可知: $\delta n_{\mathrm{I}} \geqslant \lambda/\left(2\pi l\sqrt{TN}\right)$, 此结果表明基于强度探测的折射率测量灵敏度最小值为$\lambda/\left(2\pi l\sqrt{N}\right)$, 此现象和散弹噪声极限$1/\sqrt{N}$类似。同样,将此灵敏度定义为折射率测量散弹噪声极限 RIM-SNL。原则上,直接或间接应用强度探测,折射率测量信号的灵敏度均受此极限限制。

图 2 展示了强度探测折射率测量信号灵敏度曲线及光子数和透过率对最佳灵敏度(灵敏度的最小值)的影响规律,其中 $\lambda = 532$ nm, $l = 5.3$ mm。图 2 (a) 表示信号灵敏度随介质折射率变化曲线,其中平均光子数 $N = 10$, 透过率 $T = 1$。图 2 (b) 表征了输出信号最佳灵敏度值随着光子数和透过率的变化规律。从图 2 (b) 中可以看出,信号的最佳灵敏度随着光子数的增加而升高,光子数损耗降低了信号的最佳灵敏度。

上述分析表明:通过适当增加入射光光子数 (功率) 可以提高信号的灵敏度,但是信号的分辨率却与光子数无关。增加信号透过率 (减少损耗) 可以提高信号灵敏度,但对信号的分辨率无影响。然而,增加光子数和透过率对系统性能的提升还是局限在经典的强度探测框架内,其折射率测量分辨率和灵敏度仍然受到 RIM-RDL 和 RIM-SNL 的限制,分辨率和灵敏度很难进一步提升。因此,必须革新探测体制才能突破 RIM-RDL 和 RIM-SNL 限制,提升系统探测性能。

## 4 奇偶探测折射率测量

奇偶探测最早是 Bollinger[21] 研究囚困离子时提出的,然后,Gerry 等人[22] 根据奇偶探测思想实施了相位测量,他们的研究结果突破了经典分辨率和灵敏度极限限制,实现了超分辨率和超灵敏度的相位测量。对于多数的量子态而言,奇偶探测是参数估计的最佳探测方案。奇偶探测算符$\hat{\Pi} = \mathrm{e}^{\mathrm{i}\hat{N}\pi}$ ($\hat{N} = \hat{a}^{\dagger}\hat{a}$是粒子数算符) 与魏格纳函数关系密切,确切地说魏格纳函数是位移奇偶算符的平均值,通过 MZI 输入态和输出态的魏格纳函数关系就可以计算出奇偶探测信号的平均值。对于输入态$|\alpha\rangle\langle\alpha|\otimes|0\rangle\langle 0|$,其魏格纳函数可表示为:

$$W_{\mathrm{in}}(\gamma,\beta) = W_{|\alpha\rangle}(\gamma)W_{|0\rangle}(\beta) \quad . \tag{8}$$

其中的$W_{|\alpha\rangle}(\gamma)$和$W_{|0\rangle}(\beta)$分别是相干态和真空态的魏格纳函数,它们的表达式分别为:

$$W_{|\alpha\rangle}(\gamma) = \frac{2}{\pi}\mathrm{e}^{-2|\gamma-\alpha|^2} \quad , \tag{9}$$

$$W_{|0\rangle}(\beta) = \frac{2}{\pi}\mathrm{e}^{-2|\beta|^2} \quad . \tag{10}$$

输入输出魏格纳函数间的变换关系可以用下面的变换实现:

$$W_{\mathrm{out}}(\gamma,\beta) = W_{\mathrm{in}}\left(\tilde{\gamma},\tilde{\beta}\right) \quad , \tag{11}$$

其中, $\tilde{\gamma} = \gamma\cos[\pi l(n-1)/\lambda] + \beta\sin[\pi l(n-1)/\lambda]$

$\tilde{\beta} = -\gamma\sin[\pi l(n-1)/\lambda] + \beta\cos[\pi l(n-1)/\lambda]$ .

因此,奇偶探测算符的平均值可以表示为:

$$\langle\hat{\Pi}\rangle = \frac{\pi}{2}\int_{-\infty}^{\infty} W_{\mathrm{out}}(0,\beta)\,\mathrm{d}^2\beta \quad . \tag{12}$$

考虑光子数损耗后,通过上述分析可以推导出奇偶探测信号平均值的具体表达式为

$$\langle\hat{\Pi}\rangle = \mathrm{e}^{-2TN\sin^2[\pi l(n-1)/\lambda]} \quad . \tag{13}$$

根据公式 (13), 得到了奇偶探测信号曲线,如图 3(彩图见期刊电子版)中红色点线所示,同时利用公式 (4) 绘出了强度探测信号曲线,如图 3 中黑色实线所示。从图 3 可以看出:奇偶探测信号的半最大值的全宽度 (Full Width of Half Maximum, FWHM) 明显小于强度探测的 FWHM。这

说明奇偶探测信号的分辨率优于强度探测。为了进一步给出强度探测和奇偶探测信号分辨率的定量关系，笔者利用类似小角度近似的方法将公式 (13) 做近似处理，即当$\pi l(n-1)/\lambda \ll 1$时，公式 (13) 可以近似为：

$$\left\langle \hat{\Pi} \right\rangle = \mathrm{e}^{-2TN(\pi l/\lambda)^2(n-1)^2} \quad . \tag{14}$$

通过上述近似处理可以看出此信号具有高斯分布特征，则此信号的宽度为$\Delta n_{\mathrm{P}} = \lambda/\left(2\pi l\sqrt{TN}\right)$。按照前面的讨论，强度探测信号的分辨率近似为$\Delta n_{\mathrm{I}} = \lambda/l$，当 $T = 1$ 时，强度探测信号峰比奇偶探测信号峰宽$2\pi\sqrt{N}$倍，说明奇偶探测信号的分辨率比强度探测高$2\pi\sqrt{N}$倍。因此，奇偶探测理论上可实现超越 RIM-RDL 限制的超分辨率折射率测量。

实际应用中损耗是不可避免的，图 4 给出了奇偶探测信号的 FWHM 随着透过率和光子数的变化曲线，如图中红色点线所示，其中 $\lambda = 532$ nm，$l = 1\,064$ nm。为了便于比较，图中同时给出了同条件下强度探测信号的 FWHM 随透过率和光子数的变化规律，如图中蓝色实线所示。从图中可以明显看出强度探测信号的分辨率与透过率和光子数无关，这和前面的分析结果一致。同时还可以看出，随着损耗的增加(透过率减小)和光子数的减小，奇偶探测信号分辨率降低。只有当平均光子数 $N < 1.1$ 和透过率 $T < 0.011$ 时，奇偶探测信号分辨率才低于强度探测，其余情况奇偶探测信号分辨率都远高于强度探测。因此，除了极低光子数和极高损耗的情况外，奇偶探测信号的分辨率均高于强度探测。

根据奇偶探测信号高斯误差传递公式$\delta n_{\mathrm{P}} = \sqrt{\left\langle \hat{\Pi}^2 \right\rangle - \left\langle \hat{\Pi} \right\rangle^2} \Big/ \left|\partial\left\langle \hat{\Pi} \right\rangle/\partial n\right|$可以推导出奇偶探测信号的灵敏度。首先，根据公式 (13) 及$\left\langle \hat{\Pi}^2 \right\rangle = 1$可以得到奇偶探测信号的不确定度的表达式$\Delta\Pi = \sqrt{1-\left\langle \hat{\Pi} \right\rangle^2} = \sqrt{1-\mathrm{e}^{-4TN\sin^2[\pi l(n-1)/\lambda]}}$，再计算奇偶探测信号对折射率的偏导数$\left|\partial\left\langle \hat{\Pi} \right\rangle/\partial n\right| = \dfrac{2TN\pi l}{\lambda}\left|\sin\left[\dfrac{2l\pi(n-1)}{\lambda}\right]\right|\mathrm{e}^{\left\{-2TN\sin^2\left[\frac{l\pi(n-1)}{\lambda}\right]\right\}}$，最后，通过奇偶探测高斯误差传递公式可以推导出奇偶探测信号的灵敏度表达式

$$\delta n_{\mathrm{P}} = \frac{\lambda}{2TN\pi l}\frac{\sqrt{\mathrm{e}^{4TN\sin^2[l\pi(n-1)/\lambda]}-1}}{|\sin[2l\pi(n-1)/\lambda]|} \quad . \tag{15}$$

根据公式 (15) 通过数值计算得到奇偶探测信号灵敏度曲线如图 5(彩图见期刊电子版)所示，其中 $\lambda = 532$ nm，$l = 5.3$ mm，$N = 100$。图中红色点线为奇偶探测信号灵敏度曲线。同时，为了对比分析，图中也给出了强度探测信号的灵敏度曲线，如图中蓝色实线所示。图中黑色直虚线是两条曲线的切线。两条灵敏度曲线的公切线是直线，说明两种探测方式下信号的最佳灵敏度相同。此公切线也是上述条件下折射率测量的散弹噪声极限 RIM-SNL，即奇偶探测折射率测量是以 RIM-SNL 为基础的超分辨率探测方案。

接下来考虑光子数和透过率对信号最佳灵敏度的影响。图 6(a) ~6 (b) (彩图见期刊电子版)分别给出了透过率和光子数对奇偶探测和强度探测信号最佳灵敏度的影响规律，其中 $\lambda = 532$ nm，$l = 5.3$ mm。两种探测方式下信号的最佳灵敏度均随着光子数和透过率的增加而升高，更重要的是两种情况下两条曲线始终重合，这说明两种探测的最佳灵敏度是一样的，换句话说，相较于强度探测，奇偶探测不能进一步提高折射率测量的灵敏度。

通过前面的讨论可知奇偶探测信号能够突破折射率测量衍射极限 RIM-RDL 限制，灵敏度可以达到折射率测量散弹噪声极限 RIM-SNL。然而，奇偶探测折射率测量的超分辨率物理本质还不清楚，因此，进一步分析奇偶探测超分辨率的本质是必须的，也是必要的。

文中基于强度探测和奇偶探测折射率测量所遵循的干涉原理都是以马赫-曾德尔干涉仪为基础的，输入光又均为相干态光束，因此分辨率的提升与干涉仪及输入态光束无关。那么，分辨率的提升只能与系统输出端的检测方式和后处理方法有关。强度探测是对系统输出端的光信号强度进行直接检测的传统探测方法，其分辨率依赖于经典的瑞利衍射极限，分辨率无法进一步提升。然而，奇偶探测是对输出端光信号作进一步后处理，即将输出光场的光子数进行分类，分别统计输出偶数和奇数个光子数的概率，进而给出这种奇偶性的统计分布，求出奇偶探测算符的平均值，得到奇偶探测信号。这种测量方案相当于将被测输出态投影到偶数光子数态或奇数光子数态上，即得到无限压缩量子态[23]，无限压缩态[24]是能够提高信号测量分辨率的。综上，奇偶探测信号分辨率

提升的本质就十分清楚了。这种解释类似于直接利用压缩态进行超分辨率参数估计，不同的是利用数据后处理替代了压缩态，避免了压缩态繁琐的制备环节。

## 5　结　论

文中针对传统折射率测量分辨率瓶颈问题，提出了利用奇偶探测实现超分辨率折射率测量方案。根据量子理论推导了强度探测和奇偶探测折射测量信号模型及灵敏度模型。从强度探测模型本身出发，分析其信号周期并由此定义了强度探测信号分辨率极限和灵敏度极限。通过模型分析和数值手段相结合的方式对强度探测和奇偶探测折射率测量信号进行了对比剖析，结果表明：两种探测方案的灵敏度均能达到折射率测量散弹噪声极限 RIM-SNL；奇偶探测信号分辨率远高于瑞利衍射极限，是强度探测信号分辨率的$2\pi\sqrt{N}$倍；同时，几乎在整个损耗区域内，奇偶探测分辨率均超越强度探测；最后，奇偶探测相当于把输出态投射到偶数个或奇数个光子数的无限压缩态，无限压缩必然会提高被测信号分辨率。该方案为突破经典分辨率探测极限限制开辟了道路，为超分辨率折射率测量提供了新方法。

**References:**


[1] EL-KASHEF H. Study of the refractive properties of laser dye solvents: toluene, carbon disulphide, chloroform, and benzene[J]. *Optical Materials*, 2002, 20(2): 81-86.

[2] 裴乃奇. 海水折射率测量系统优化和实验研究[D]. 武汉: 华中科技大学, 2017.
PEI N Q. Optimization and experiment on seawater's refractive index measurement system[D]. Wuhan: Huazhong University of Science and Technology, 2017. (in Chinese)

[3] INDRASARI W, UMIATIN U, FITRIANI N. Measurement system development of refractive index, salinity and magnetic field parameters on liquid waste polluted water[J]. *Journal of Physics:Conference Series*, 2021, 1869: 012201.

[4] CONTEDUCA D, BARTH I, PITRUZZELLO G, *et al*.. Dielectric nanohole array metasurface for high-resolution near-field sensing and imaging[J]. *Nature Communications*, 2021, 12(1): 3293.

[5] 张静. 迈克尔逊等倾干涉法晶体折射率测量方法研究[D]. 济南: 山东大学, 2009.
ZHANG J. Measurement of crystal refractive index based on Michelson interferometry[D]. Ji'nan: Shandong University, 2009. (in Chinese)

[6] HU Y, LV J H, HAO Q. Refractive index measurement of glass with arbitrary shape based on Brewster's law and a focusing probe beam[J]. *Sensors*, 2021, 21(7): 2421.

[7] 付兴丽, 冯杰, 范晓辉, 等. 基于最小偏向角法的高精度液体折射率测量装置的优化设计与测量研究[J]. 中国光学（中英文）, 2022, 15(4): 789-796.
FU X L, FENG J, FAN X H, *et al*.. Optimization design and test of a high-precision measuring device of liquid refractive index based on the method of minimum deviation angle[J]. *Chinese Optics*, 2022, 15(4): 789-796. (in Chinese)

[8] LI G Q, CEN X, SU J, *et al*.. Fabry-Perot cavity enhanced Prism for highly sensitive refractive index measurement of Water[J]. *Optik*, 2021, 245: 167688.

[9] 王文生, 徐斌, 张军. 最小偏向角法V棱镜法测量折射率的原理公式误差[J]. 长春光学精密机械学院学报, 1995, 18(1): 5-10.
WANG W SH, XU B, ZHANG J. The principle formula error of measuring the refractive index by the method of minimum deviation angle and the method of V-prism[J]. *Journal of Changchun Institute of Optics and Fine Mechanics*, 1995, 18(1): 5-10. (in Chinese)

[10] IDRIS N, MASWATI, YUSIBANI E. The effect of the thickness of the glass plate of a hollow prism on the accuracy of measuring the refractive index of edible oil[J]. *Optik*, 2020, 217: 164834.

[11] 刘金秋, 郑运强, 杨雪梅, 等. 基于劈尖的等厚干涉测量氯化钾和酚酞的折射率[J]. 科技风, 2020(21): 105.
LIU J Q, ZHENG Y Q, YANG X M, *et al*.. Measurement of refractive index of potassium chloride and phenolphthalein by wedge interferometry[J]. *The Wind of Science and Technology*, 2020(21): 105. (in Chinese)

[12] 杜登熔, 李艳, 商成林, 等. 利用迈克尔逊干涉仪测量液体的折射率[J]. 大学物理实验, 2019, 32(1): 43-45.
DU D R, LI Y, SHANG CH L, *et al*.. Measurement of liquid refractive index by Michelson interferometer[J]. *Physical*

*Experiment of College*, 2019, 32(1): 43-45. (in Chinese)

[13] SANJID M A, CHAUDHARY K P. Measurement of refractive index of liquids using length standards traceable to SI unit[J]. *MAPAN*, 2016, 31(2): 89-95.

[14] STONE J, EGAN P, GERTY D, *et al*.. Picometer metrology for precise measurement of refractive index, pressure, and temperature[J]. *NCSLI Measure*, 2013, 8(4): 67-73.

[15] 张丽颖, 顾菊观. 基于Mathematica的牛顿环干涉与折射率关系的讨论[J]. 广西物理, 2021, 42(1): 28-32.
ZHANG L Y, GU J G. Discussion on relation between Interference and refractive index of Newtonian rings based on Mathematica[J]. *Guangxi Physics*, 2021, 42(1): 28-32. (in Chinese)

[16] 魏方皓, 张祥军, 唐守锋. 基于表面等离子体共振的光子晶体光纤折射率传感器的设计与分析[J]. 半导体光电, 2020, 41(1): 35-38,43.
WEI F H, ZHANG X J, TANG SH F. Design and analysis of photonic crystal fiber refractive index sensor based on surface Plasmon resonance[J]. *Semiconductor Optoelectronics*, 2020, 41(1): 35-38,43. (in Chinese)

[17] 张好运, 赵海涵, 徐昕阳, 等. 基于光学频率梳光谱干涉实现水的群折射率测量[J]. 激光与红外, 2020, 50(7): 781-788.
ZHANG H Y, ZHAO H H, XU X Y, *et al*.. Measurement of water refractive index by dispersive interferometry[J]. *Laser & Infrared*, 2020, 50(7): 781-788. (in Chinese)

[18] CHOI H J, LIM H H, MOON H S, *et al*.. Measurement of refractive index and thickness of transparent plate by dual-wavelength interference[J]. *Optics Express*, 2010, 18(9): 9429-9434.

[19] BOTO A N, KOK P, ABRAMS D S, *et al*.. Quantum interferometric optical lithography: exploiting entanglement to beat the diffraction limit[J]. *Physical Review Letters*, 2000, 85(13): 2733-2736.

[20] 张兴超, 潘锐, 韩嘉悦, 等. 拓扑量子材料光电探测器研究进展[J]. 中国光学, 2021, 14(1): 43-65.
ZHANG X CH, PAN R, HAN J Y, *et al*.. Recent progress and prospects of topological quantum material-based photodetectors[J]. *Chinese Optics*, 2021, 14(1): 43-65. (in Chinese)

[21] BOLLINGER J J, ITANO W M, WINELAND D J, *et al*.. Optimal frequency measurements with maximally correlated states[J]. *Physical Review A*, 1996, 54(6): R4649-R4652.

[22] GERRY C C. Heisenberg-limit interferometry with four-wave mixers operating in a nonlinear regime[J]. *Physical Review A*, 2000, 61(4): 043811.

[23] DISTANTE E, JEŽEK M, ANDERSEN U L. Deterministic superresolution with coherent states at the shot noise limit[J]. *Physical Review Letters*, 2013, 111(3): 033603.

[24] ANISIMOV P M, RATERMAN G M, CHIRUVELLI A, *et al*.. Quantum metrology with two-mode squeezed vacuum: parity detection beats the Heisenberg limit[J]. *Physical Review Letters*, 2010, 104(10): 103602.

Author Biographics:

Wang Qiang (1980—), male, born in Baiquan, Heilongjiang Province, Ph.D., associate professor, master student supervisor. In 2006 and 2016, he obtained master degree and Ph.D. degree from Harbin Institute of Technology, respectively. He is currently engaged in research on quantum interference metrology and sensing, quantum lidar, etc. E-mail: wangqiang8035@163.com

王强 (1980—), 男, 黑龙江拜泉人, 博士, 副教授, 硕士生导师, 2006 年、2016 年于哈尔滨工业大学分别获得硕士、博士学位, 主要从事量子干涉度量及传感, 量子激光雷达等方面的研究。E-mail: wangqiang8035@163.com

Hao Li-li (1981 —), female, born in Suihua, Heilongjiang Province, Ph.D., associate professor, master student supervisor. She received her master degree and Ph.D. degree from Harbin Institute of Technology in 2007 and 2015 respectively, mainly engaged in the research of quantum optics, spatial optical solitons and optical control devices. E-mail: haolili0820@126.com

郝利丽 (1981—), 女, 黑龙江绥化人, 博士, 副教授, 硕士生导师, 2007 年、2015 年分别于哈尔滨工业大学获得硕士、博士学位, 主要从事量子光学, 空间光孤子及光控器件等方面的研究。E-mail: haolili0820@126.com